Polyhedron 206 (2021) 115324

Contents lists available at ScienceDirect

Polyhedron

journal homepage: www.elsevier.com/locate/poly

Structure-property studies of a new {$Fe^{III}_2Mn^{II}$} complex☆

Nigam P. Rath [a,b], Stephen M. Holmes [a,b,*]

[a] Department of Chemistry and Biochemistry, University of Missouri-St. Louis, St. Louis, MO 63121, USA
[b] Center for Nanoscience, University of Missouri-St. Louis, St. Louis, MO 63121, USA

ARTICLE INFO

Keywords:
Cyanometalates
Crystal structures
Magnetic properties
Polynuclear complexes

ABSTRACT

The preparation, structure, and magnetic properties of a trinuclear complex, {[(Tp*)Fe^{III}(CN)$_3$]$_2$[Mn^{II}(phen)$_2$]} (**1**), are described. The trinuclear complex is obtained via treatment of dimethylformamide/diethyl ether mixtures of [NEt_4][(Tp*)Fe^{III}(CN)$_3$]·H_2O [Tp* = tris(3,5-dimethylpyrazolyl)borate], manganese(II) trifluoromethanesulfonate, and two equivalents of 1,10-phenanthroline. Analysis of the magnetic data suggests that **1** contains a 2:1 ratio of low spin Fe^{III}_{LS} (S = ½) and high spin Mn^{II}_{HS} ($S = {}^5/_2$) ions that undergo cyanide-mediated antiferromagnetic exchange within the Fe^{III}_{LS}(μ-CN)Mn^{II}_{HS} units. Overall, an $S = {}^3/_2$ magnetic ground state is found for the complex, with J_{iso} = -6.9(1) cm^{-1} and g_{iso} = 2.11(1).

1. Introduction

The rational design and synthesis of polynuclear cyanide-bridged complexes continue to enjoy world-wide interest across chemistry, physics, and materials science communities. In these complexes unquenched orbital angular momentum may be exploited to construct materials that under ideal circumstances display slow magnetic relaxation dynamics [1–4]. Among more facile synthons for their construction, are a class of tricyanometalates containing tridentate capping ligands known as poly(pyrazolyl)borates (Tp^R), specifically those containing [(Tp^R)Fe^{III}(CN)$_3$]$^-$ anions [1–12].

Tricyanopyrazolylborates are a versatile class of paramagnetic complexes for engineering of polynuclear derivatives [2–37]. The facially-coordinate tripodal ligands may be systematically modified at up to ten positions allowing for selective control of their steric demand and donor properties [1,2,38]. These ligands are known to support a variety of transition metal centers and allow for selective tuning of their redox properties over wide potential windows [3,30,31,38]. More specifically, the steric demand of the pyrzolylborates in [(Tp^R)Fe^{III}(CN)$_3$]$^-$ anions limit the numbers and directionality of formed cyanide bridges during self-assembly reactions, allowing simultaneous control of solubility and nuclearity of cluster derivatives. These include a variety of tri- [2–4,6–14], tetra- [2,4,15–21,32], hexa- [2,22], octa- and nonanuclear complexes [22–29] and chains [33–37], whose properties include slow magnetic relaxation [2–4,9–13,15–25,33–37] and photoresponsive [28–32,35–37,39–47] behavior.

In a continuing effort, to explore the relationship between magnetic anisotropy and the creation of energy barriers to magnetic spin reversal, we turned our attention to polynuclear complexes containing divalent manganese centers. We previously discovered that the relative orientations of the three-fold rotation axes (B···Fe vectors) in clusters containing [(Tp^R)Fe^{III}(CN)$_3$]$^-$ anions are reasonable structural markers for anisotropy tensors in polynuclear Fe^{III}/Ni^{II} complexes. Slow magnetic relaxation is often strongly correlated with colinear arrangements of these axes which generally leads to the observation of single-molecule magnetism [2,3,10–13,18,22,24-26,48,49]. Under ideal circumstances the Fe^{III}_{LS} centers provide first-order and unquenched orbital angular momentum to the magnetic spin ground state and lead to respectable energy barriers to spin reversal [2,3,48,49].

While considerable efforts have focused on cyanide-bridged Fe^{III}/Ni^{II} clusters comparatively less has concerned the preparation of soluble Fe/Mn analogues. These complexes are of potential interest as they may afford odd integer spin ground states that discourage quantum tunneling of the magnetization, potentially leading to higher barriers to magnetization reversal [2–12]. A secondary consideration is that these clusters may also serve as soluble model complexes for understanding how to control optical and magnetic bistability seen in three-dimensional Fe/Mn Prussian blues [50–56]. In these solids, reversible interconversion of Fe^{III}_{LS}/Mn^{II}_{HS} and Fe^{II}_{LS}/Mn^{III}_{HS} pairs are seen, that are associated with dramatic changes in metrical parameters (cubic ↔ tetragonal) related to the introduction of Jahn-Teller distorted Mn^{III}_{HS} ions [50–56]. Surprisingly, while numerous bistable three-dimensional networks [50–56],

☆ Part of the special issue dedicated to the element manganese, entitled Manganese: A Tribute to Chemical Diversity.

* Corresponding author at: Department of Chemistry and Biochemistry, University of Missouri-St. Louis, St. Louis, MO 63121, USA.
E-mail address: holmesst@umsl.edu (S.M. Holmes).

https://doi.org/10.1016/j.poly.2021.115324
Received 3 May 2021; Accepted 7 June 2021
Available online 11 June 2021

chains [57–63], and complexes [2,4,15,45,46,64] are known for cyanide-bridged Fe/Co pairs, only one example of intramolecular electron transfer is reported for a Fe/Mn cluster under electrochemical conditions [27]. We now describe recent efforts to prepare new magnetic cyanide-bridged Fe/Mn complexes.

1.1. General considerations

All operations were conducted under an argon atmosphere using standard Schlenk and dry box techniques. Solution transfers utilized stainless steel cannulas. The preparation of $[NEt_4][(Tp^*)Fe^{III}(CN)_3]\cdot H_2O$ [Tp* = tris(3,5-pyrazolylborate] [15,16] and manganese(II) trifluoromethanesulfonate $[Mn(OTf)_2]$ [65] are described elsewhere. 1,10-phenanthroline (Acros) and $NaBPh_4$ (Acros) were used as received. Diethyl ether (Na/benzophenone) and dimethylformamide (VAC Atmospheres, activated alumina column) were dried and sparged with argon prior to use. Elemental analyses were performed by Robertson Microlit Laboratories.

Caution! Although no problems were encountered during our studies cyanides are toxic and should be handled with care.

1.2. Preparation of $\{[(Tp^*)Fe(CN)_3]_2[Mn(phen)_2]\}\cdot 2DMF$ (1)

Solid $Mn(OTf)_2$ (0.1151 g, 0.326 mmol) and 1,10-phenanthroline (73.4 mg, 0.408 mmol) were combined as solids, dissolved into DMF (5 mL) and magnetically stirred for 10 min. After $NaBPh_4$ (0.2359 g, 0.689 mmol) addition a yellow solution was obtained. $[NEt_4][(Tp^*)Fe(CN)_3]\cdot H_2O$ (0.1901 g, 0.328 mmol) was partially dissolved into DMF (5 mL) and was slowly added to the stirred Mn/phen solution (ca. 30 s) to afford an orange-red mixture. An additional volume of DMF (3 mL) was added to dissolve a small quantity of solid after 5 min. Subsequent Et_2O (30 mL) addition gave a cloudy mixture that was allowed to stand at room temperature (29 °C) overnight. After standing an additional 7 d at 15 °C, the dark red-brown crystals (**1** + **2DMF**) were collected via suction filtration, washed with Et_2O (2 × 5 mL), and dried under vacuum for 30 s at room temperature (29 °C). Yield: 150.1 mg (64.3%). Anal. Calcd for $C_{66}H_{78}N_{24}B_2Fe_2MnO_2$ (**1** + **2DMF**): C, 55.52; H, 5.51; N, 23.55. Found: C, 55.10; H, 5.24; N, 23.22. IR (Nujol/KBr, cm^{-1}): 2540 (w), 2145 (s), 2136 (s), 2118 (w), 2085 (m), 1674 (vs). Crystals of **1** + **2DMF** are readily desolvated upon prolonged standing in Et_2O to give **1** as hygroscopic crystals.

1.3. Spectroscopic and magnetic measurements

Infrared spectra were recorded as Nujol mulls between KBr plates on a Thermo-Fisher Nicolet Impact 6700 FTIR instrument in the 400–4000 cm^{-1} region. Magnetic measurements using a microcrystalline sample of **1** (57.8 mg) were collected on a Quantum Design PPMS9 magnetometer operating between 1.8 and 298 K and applied magnetic fields ranging between $0 \leq H_{dc} \leq 7$ T. The magnetic data were corrected for the sample holder and diamagnetic contributions were estimated using Pascal's constants [66]. Elemental analysis was performed by Robertson Microlit Laboratories. Magnetic data figures were generated using Origin 2020 (www.originlab.com).

1.4. Structural determinations and refinements

Single crystal structural data for **1** and **1** + **2DMF** were collected at 290(2) and 100(2) K on a Bruker D8 Venture-Duo PHOTON-II Kappa CCD diffractometer using graphite-collimated MoKα (λ = 0.71073 Å) radiation. All crystals were mounted in Paratone-N oil on nylon loops. The structures were solved by direct methods (SHELXS2014) [67,68] and completed by difference Fourier methods (SHELXL-2016) [67,68]. Refinement was performed against F^2 by weighted full-matrix least-squares (SHELXL-2016) [67,68] and empirical absorption corrections (SADABS) [69] were applied. Hydrogen atoms for **1** and **1** + **2DMF** were found in difference maps and subsequently placed at calculated positions using suitable riding models with isotropic displacement parameters derived from their carrier atoms. Non-hydrogen atoms were refined with anisotropic displacement parameters. Atomic scattering factors were taken from the *International Tables for Crystallography Vol. C. 82* [70]. All figures were generated using CrystalMaker X® (CrystalMaker Software Ltd, www.crystalmaker.com).

1.5. Synthesis and crystallographic Studies.

A new trinuclear complex, $\{[(Tp^*)Fe(CN)_3]_2[Mn(phen)_2]\}$ (**1**), is readily obtained via sequential treatment of manganese(II) trifluoromethanesulfonate with 1,10-phenanthroline, followed by sodium tetraphenylborate and $[NEt_4][(Tp^*)Fe(CN)_3]\cdot H_2O$. Efforts to obtain **1** using 2:1 ratios of iron(III) and manganese(II) salts consistently yielded a mixture of products. X-ray quality crystals of **1** are obtained from DMF/Et_2O mixtures to give a solvated complex (**1** + **2DMF**). The solvated crystals display two intense cyanide stretching absorptions [2145 and 2136 cm^{-1}] in its infrared spectrum that are shifted to higher energies relative to those seen for $[NEt_4][(Tp^*)Fe(CN)_3]\cdot H_2O$ (2119 cm^{-1}) and $[NEt_4]CN$ (2056 cm^{-1}) [15,16,65]. These correspond to bridging cyanides and are in the range expected for polynuclear complexes containing Fe^{III}-CN-Mn^{II} linkages [2,4,6–8,15,16,27,59–64]. The lower energy and weaker intensity ν_{CN} stretches [2118 and 2085 cm^{-1}] are consistent with the presence of terminal cyanides, as the intermediate energy one is nearly identical to that in $[NEt_4][(Tp^*)Fe(CN)_3]\cdot H_2O$ [15,16]. While the lowest energy absorption [2085 cm^{-1}] initially suggested terminal Fe^{II}_{LS}-CN units may be present, subsequent magnetic measurements (*vide infra*) show this is unlikely, and we tentatively attribute the unusual energy to crystal packing effects in the solid state [50–57]. Consistent with this assumption, we observe a single ν_{BH} absorption [2540 cm^{-1}] that is in the range expected for cyanide-bridged clusters derived from trivalent $[(Tp^*)Fe^{III}(CN)_3]^-$ and manganese(II) centers [2,15,16]. Lattice DMF is also confirmed in solid samples of **1** + **2DMF** via an intense ν_{CO} [1674 cm^{-1}] absorption while this absorption remains absent in the infrared spectrum of **1** [71].

Complexes **1** and **1** + **2DMF** are found in the tetragonal $I4_1/a$ space group [Table 1 and Figs. 1 and S1]. The neutral trinuclear $\{Fe^{III}_2Mn^{II}\}$ complexes contain a central $[cis\text{-}Mn^{II}(phen)_2(\mu\text{-}NC)_2]$ fragment that is linked to two adjacent and crystallographically equivalent trivalent iron centers via bridging cyanides, leaving two terminal ones per iron site. The average Fe^{III}-C and Fe^{III}-N distances for **1** [1.910(8) and 2.005(6) Å] and **1** + **2DMF** [1.919(7) and 2.000(5) Å] are nearly identical (Table 2).

Table 1
Crystallographic data for **1** and **1** + **2DMF**.[a-c]

Cmpd.	**1**	**1** + **2DMF**
Formula	$C_{60}H_{60}N_{22}B_2Fe_2Mn$	$C_{66}H_{74}N_{24}B_2Fe_2MnO_2$
Formula weight	1277.56	1423.75
λ (Å)	0.71073	0.71073
T (K)	290(2)	100(2)
Crystal system	tetragonal	tetragonal
Space group	$I4_1/a$	$I4_1/a$
a (Å)	19.531(3)	20.008(2)
b (Å)	19.531(3)	20.008(2)
c (Å)	36.740(5)	34.836(4)
α()	90	90
β (Å)	90	90
γ(Å)	90	90
V (Å^3)	14014(5)	13946(4)
Z	8	8
ρ_{calcd} (mg m^{-3})	1.211	1.356
μ (mm^{-1})	0.638	0.651
R_1[b]	0.0745	0.0750
wR_2[c]	0.1663	0.1758

[a] $I \geq 2\sigma(I)$.
[b] $R_1 = \sum||F_o| - |F_c||/\sum|F_o|$.
[c] $wR_2=\{\sum[w(F_o^2\text{-}F_c^2)^2]/\sum[w(F_o^2)^2]\}^{1/2}$.

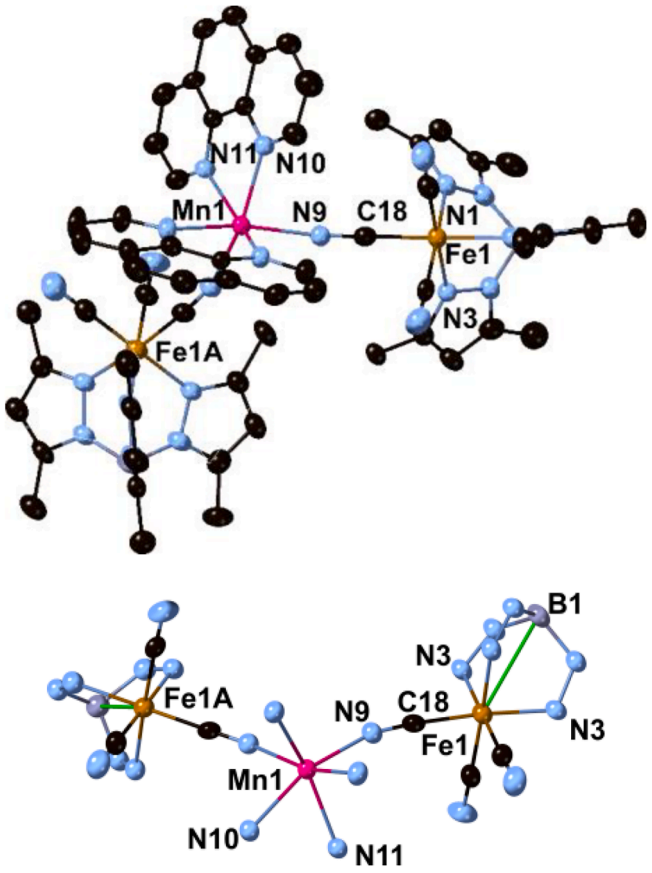

Fig. 1. (top) X-ray structures of **1**. Thermal ellipsoids are at the 50% level and hydrogen atoms are eliminated for clarity. (bottom) Truncated X-ray structure of **1** highlighting the C_3 rotation axes (green lines) that are colinear with the B···Fe anisotropy vectors. Thermal ellipsoids are at the 50% level.

Likewise, the Mn^{II}-N bonds are similar, ranging between 2.166(6) and 2.300(5) Å [Mn1-N9A and Mn1-N11] in **1**, while those in the solvate are slightly shorter [2.176(6) and 2.263(5) Å; Mn1-N7 and Mn1-N11]. The $Mn1\text{-}N_{phen}$ bonds located *trans* to the bridging cyanides [Mn1(μ-NC)Fe units] are comparable to those in several Fe^{III}/Mn^{II} complexes [2,4,72–76].

The phenanthroline N-Mn1-N bite angles are rather acute [73.1(2) and 72.5(2)°] while those involving the *cis*-cyanides [98.0(3) and 97.0 (3)°] are considerably larger. The Mn1-NC cyanide angles deviate significantly from linearity [160.5(5) and 163.3(6)°] while the Fe-CN ones remain nearly linear, for **1** and **1** + **2DMF**, respectively. In solvated crystals (**1** + **2DMF**) the DMF molecules are located within channel voids that lie along the crystallographic *a*-direction. These channels are formed via close contacts between six adjacent clusters [Fig. 2 and S2–S4], where the $[Mn(phen)_2]^{2+}$ fragments are proximal to other clusters, via their coordinated Tp* ligands [Fig. 2]. The Mn···Mn [14.23(1) Å] and phen···phen distances [10.76(1) Å] are remote while the Tp*···Tp* ring separations [5.38(1) and 10.57(1) Å] vary considerably; the Tp*···phen ones are considerably shorter [3.63(1) and 8.38(1) Å]. Overall these close intermolecular contacts lead to the creation of substantially large channel volumes (ca. 19%) where lattice solvent (i.e. DMF) may be easily accommodated.

1.6. Magnetic studies

The static and dynamic properties of **1** have been evaluated between 1.8 and 300 K. At room temperature, the temperature dependence of the χT vs T data under an applied magnetic field of 1 T shows that a 2:1 ratio of non-interacting paramagnetic Fe^{III}_{LS} ($S = ½$) and Mn^{II} ($S = {}^5/_2$) sites

Table 2
Selected bond distances (Å) and angles (°) for **1** and **1** + **2DMF**.

1		**1** + **2DMF**	
Fe1-C16	1.940(8)	Fe1-C16	1.904(7)
Fe1-C17	1.888(9)	Fe1-C17	1.928(8)
Fe1-C18	1.901(8)	Fe1-C18	1.925(7)
Fe1-N1	1.990(6)	Fe1-N2	2.000(5)
Fe1-N3	2.016(5)	Fe1-N4	2.001(5)
Fe1-N5	2.008(6)	Fe1-N6	1.998(5)
Mn1-N9A	2.166(6)	Mn1-N7	2.176(6)
Mn1-N10	2.276(5)	Mn1-N10	2.260(6)
Mn1-N11	2.300(5)	Mn1-N11	2.263(5)
C16-N7	1.147(8)	C16-N7	1.168(8)
C17-N8	1.166(9)	C17-N8	1.151(8)
C18-N9	1.174(7)	C18-N9	1.155(8)
C16-Fe1-C17	89.5(3)	C16-Fe1-C17	86.5(3)
C16-Fe1-C18	85.6	C16-Fe1-C18	87.0(3)
C17-Fe1-C18	85.9(3)	C17-Fe1-C18	88.0(3)
C16-Fe1-N1	177.8(3)	C16-Fe1-N2	92.4(2)
C16-Fe1-N3	90.0(3)	C16-Fe1-N4	92.6(2)
C16-Fe1-N5	91.5(2)	C16-Fe1-N6	177.0(2)
N1-Fe1-N3	89.0(3)	N2-Fe1-N4	89.1(2)
N1-Fe1-N5	90.5(2)	N2-Fe1-N6	89.6(2)
N3-Fe1-N5	89.4(2)	N4-Fe1-N6	89.7(2)
N9-Mn1-N9A	97.0(3)	N7-Mn1-N7A	98.0(3)
N9-Mn-N10	84.4(2)	N7-Mn-N10	85.2(2)
N9-Mn1-N10A	160.9(2)	N7-Mn1-N10A	163.8(2)
N9-Mn1-N11	108.2(2)	N7-Mn1-N11	100.2(2)
N9-Mn1-N11A	88.6(2)	N7-Mn1-N11A	90.7(2)
N10-Mn1-N10A	96.4(3)	N10-Mn1-N10A	96.2(2)
N10-Mn1-N11	72.5(2)	N10-Mn1-N11	73.1(2)
N10-Mn1-N11A	90.6(2)	N10-Mn1-N11A	95.7(2)
N11-Mn1-N11A	154.9(3)	N11-Mn1-N11A	163.5(3)
Fe1-C16-N7	178.3(7)	Fe1-C16-N7	176.9(6)
Fe1-C17-N8	179.2(8)	Fe1-C17-N8	177.4(6)
Fe1-C18-N9	175.4(6)	Fe1-C18-N9	179.5(7)
Mn1-N9-C18	163.3(6)	Mn1-N7-C16	160.5(5)

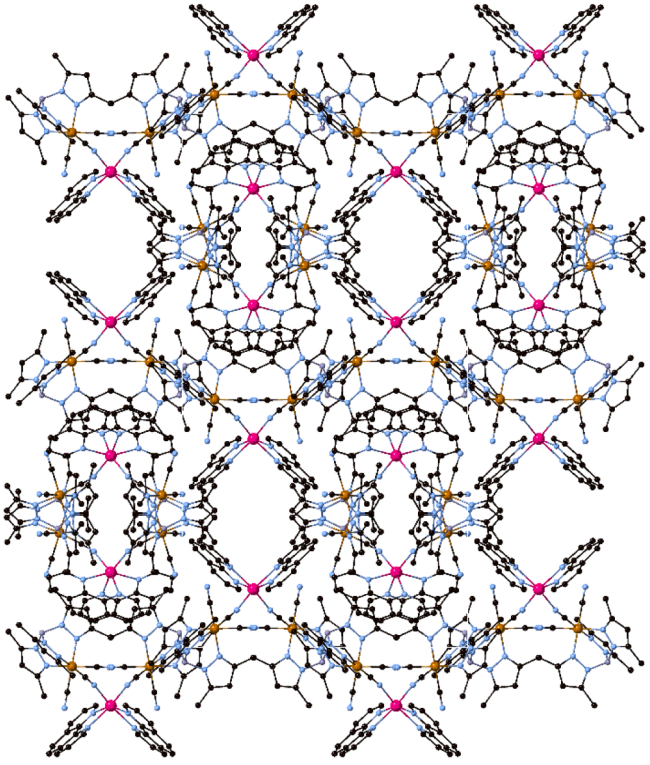

Fig. 2. Packing diagram of **1** viewed along the crystallographic (top) *a*-direction. Hydrogen atoms are eliminated for clarity.

are present and that orbital contributions from the Fe^{III}_{LS} (S = ½) spin states are largely quenched [Fig. 3]. At 298 K the χT product [5.56 cm^3 K mol^{-1}] is close to the expected value, while those between 298 and 58 K, decrease slightly, and then rapidly approach a minimum of 2.25 cm^3 K mol^{-1} at 1.8 K. This behavior is reminiscent of several polynuclear $Fe^{III}_{LS}/Mn^{II}_{HS}$ clusters that undergo antiferromagnetic superexchange interactions [61–69].

Given the trinuclear structure of **1**, the χT vs T data were initially fitted using an isotropic Heisenberg Hamiltonian [Eqn. 1]. Under weak-field conditions, where J represents an isotropic exchange interaction between adjacent Fe^{III}_{LS} ($S_{Fe1} = S_{Fe1A}$ = ½) and Mn^{II}_{HS} ($S_{Mn} = {}^5/_2$) sites, and S_i represents the spin operators for each metal center [8], the following equations were considered:

$$H = -2J[S_1 \cdot S_2 + S_2 \cdot S_3] - 2\,J' S_1 \cdot S_2 \quad (1)$$

$$\chi_m = N_A g^2 \beta^2 / 4kT(A/B) \quad (2)$$

$$A = 35 + 10e^{(-7J/kT)} + 35e^{(-2J/kT)} + 84e^{(5J/kT)} \quad (3)$$

$$B = 3 + 2e^{(-7J/kT)} + 3e^{(-2J/kT)} + 4e^{(5J/kT)} \quad (4)$$

Under the assumption that magnetic anisotropy and dipolar intermolecular interactions may complicate our analysis at low temperatures, the magnetic susceptibility data was fitted above 10 K [eqns. 2–4], leading to estimated values of g = 2.11(1) and J = -6.9(1) cm^{-1} [Fig. S5]. Subsequent fitting of the χT vs T data above 10 K using PHI [77] gave comparable values [2.05(1) and −9.8(1) cm^{-1}] [Fig. S6].

The estimated exchange parameter for **1** is slightly larger than those reported for some other complexes, which may be attributed to the greater single-ion anisotropy and electron density delocalization brought by the $[(Tp^*)Fe^{III}(CN)_3]^-$ anion [2,3,12,13,22,29]. This observation is consistent with the expectation that spin density is efficiently communicated in accordance with orbital symmetries and exchange interactions predicted via Goodenough-Kannomori rules [10,15,16,78]. For example, Zuo and You report moderate anisotropy in linear $\{[(Tp)Fe^{III}(CN)_3]_2[Mn^{II}(MeOH)_4]\}\cdot 2MeOH$ [g = 2.13; J = -2.19 cm^{-1}] [6], where Tp = tris(pyrazolyl)borate, while Kim suggests larger g and J parameters are seen [g = 2.22(1) and J = -7.6(2) cm^{-1}] [64]. In comparison, bent trinuclear $\{[(pcq)Fe^{III}(CN)_3]_2[Mn(L)_{4-n}]\}\cdot n$(solvent) analogues, where pcq^- = 8-(pyridine-2-caboxamido)quinoline, relatively small intra- and intermolecular exchange parameters are seen. Complex $\{[(pcq)Fe(CN)_3]_2[Mn(MeOH)_2(OH_2)_2\}\cdot 2H_2O$ is nearly isotropic [g = 2.05(1); J and zJ = -1.11(6) and −0.39(2) cm^{-1}], while slightly larger g and J terms are seen for $\{[(pcq)Fe(CN)_3]_2[Mn(L)_2]\}\cdot MeOH\cdot 2H_2O$ analogues [g = 2.06(1) and 2.05(1); J = -3.73(3) and −4.03(3) cm^{-1}; zJ = -0.17(1) and −0.15(1) cm^{-1}], when L = bipyridine (bpy) and 1,10-phenanthroline (phen), respectively [7]. Likewise, small g and J values are found for $\{[Fe(bpy)(CN)_4]_2[Mn(OH_2)_4]\}\cdot 4H_2O$ [g = 2.0; $J_{Fe\text{-}Mn}$ = -1.3 cm^{-1} and $J_{Fe\text{-}Fe}$ = -0.87 cm^{-1}] [79]. Similarly, dinuclear $\{[Fe(bpb)(CN)_2][Mn(phen)_2Cl]\}\cdot 5MeOH\cdot 1.5H_2O$ [g = 2.01(1); J = -2.68(3) cm^{-1}], where bpb^{2-} = 1,2-bis(pyridine-2-carboxamido)benzenate] [7], tetranuclear $\{[(Tp)Fe(CN)_3]_2[Mn(bpy)_2]_2[ClO_4]_2\}\cdot 4MeCN$ [g = 2.10 (1); J_1 and J_2 = -2.29(3) and −0.76(1) cm^{-1}] [6], and pentanuclear $\{[Mn_3(MAC)_3(OH_2)_2][Fe(CN)_6]_2\}\cdot 6H_2O\cdot 2MeOH$ (MAC = 2,13-dimethyl-3,6,9,12,18-pentaazabicyclo[12.3.1]octadeca-1 (18),2,12,14,16-pentaene) [g = 2.03 and $J \sim -2$ cm^{-1}] [80] exhibit smaller exchange parameters and orbital contributions to their magnetic ground states.

The field dependence of the magnetization was measured at various applied magnetic fields and temperatures to better assess the magnetic properties of **1**. The M vs H data clearly shows that **1** nearly saturates approaching a maximum value of 5.24 μ_B at 1.9 K [Inset of Figs. 3 and S7]. The experimental value is close to the one expected [5.68 μ_B with $g_{iso} \sim 2.1$] for a 2:1 ratio of antiferromagnetically coupled Fe^{III}_{LS} (S = ½) and Mn^{II}_{HS} ($S = {}^5/_2$) ions, adopting an overall $S = {}^3/_2$ spin ground state. Assuming that **1** possess Ising-like magnetic anisotropy (for $D < 0$) and considering the Hamiltonian $H = DS^2_{T(z)}$ [eqn. 5], the expected spin reversal energy barrier should scale as $U_{eff} = |D|$ (S^2_T – ¼) rather than $|D|$ S^2_T [23,81], given the half-integer spin ground state of **1**. To investigate this hypothesis, we performed a series of calculations using PHI [77] where fitting of the M vs H data [Fig. S8] gave an estimated value of $|D|$ = 4.5 cm^{-1} for **1**. This leads to a prediction of a rather small spin reversal barrier [U_{eff} = 9 cm^{-1}] for the $\{Fe^{III}_2Mn^{II}\}$ cluster [6–8,64].

Nevertheless, we remained hopeful that **1** would display slow relaxation dynamics given its structural similarity to other trinuclear $\{Fe^{III}_2M^{II}\}$ single-molecule magnets. In trinuclear $\{Fe^{III}_2Ni^{II}\}$ complexes the observation of slow magnetization relaxation dynamics is strongly correlated with the presence of linear Fe^{III}-CN-Ni^{II} bridges and a colinear alignments of its magnetic anisotropy tensors (i.e. B···Fe; C_3 rotation axes) [2,3,48,49]. In the present case, bent Mn-NC units [160.5(5)°] are seen and the B···Fe vectors adopt a ca. 62.9(1)° orientation relative to each other [Figs. 1 and S4]. Unfortunately, these factors often quench orbital contributions to the magnetic spin ground state and bring insufficient magnetic anisotropy to the complex. Consistent with this assumption, we were unable to observe any frequency-dependent behavior in the ac susceptibility data, confirming that rapid quantum tunneling and/or efficient mixing of the ground and low-lying excited states conspire to give exceptionally small barriers to magnetic relaxation in **1**.

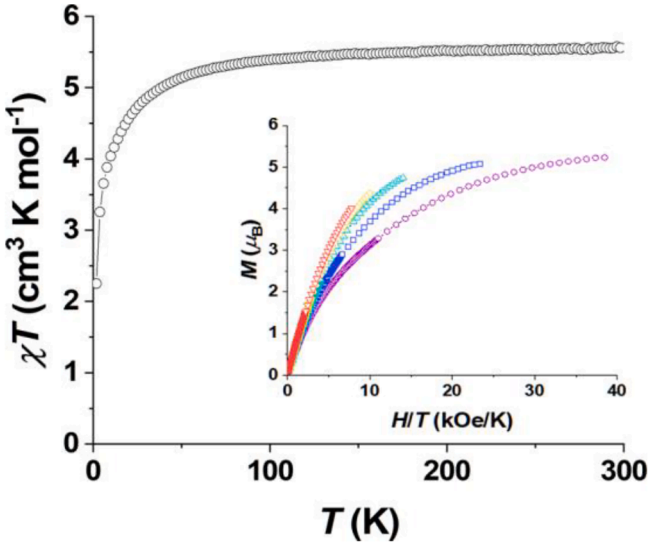

Fig. 3. Temperature dependence of the χT product for **1** under a static applied dc magnetic field of H = 1 T. Inset: M vs H T^{-1} data for **1** collected at 1.9 (○), 3 (□), 5 (△), 7 (◇), and 9 (▽) K. The lines are guides for the eye.

2. Conclusions

The preparation, structure, and magnetic properties of a cyanide-bridged trinuclear $\{Fe^{III}_2Mn^{II}\}$ complex is described. Owing to the presence of numerous close intermolecular contacts and highly bent Fe (μ-CN)Mn linkages only modest antiferromagnetic exchange interactions are seen. Astonishingly, despite favorable redox potentials for the iron and manganese sites, intramolecular electron transfer remains absent in **1**. We attribute this behavior to its distorted structure which provides an inadequate ligand field for facile electron transfer within the Fe^{III}(μ-CN)Mn^{II} units.

CRediT authorship contribution statement

Nigam P. Rath: Methodology, Validation, Formal analysis, Investigation, Resources, Data curation, Visualization, Supervision. **Stephen M. Holmes:** Conceptualization, Methodology, Validation, Formal analysis, Investigation, Resources, Data curation, Visualization,

Supervision, Project administration, Funding acquisition.

Declaration of Competing Interest

The authors declare that they have no known competing financial interests or personal relationships that could have appeared to influence the work reported in this paper.

Acknowledgements

S.M.H. gratefully acknowledges the National Science Foundation (CHE-1214063 and CHE-1800578; CHE-1827756, X-ray; CHE-1800578, supplemental support-helium reliquefier) and the University of Missouri-St. Louis for financial support. S.M.H. also thanks Anthony Caruso for the loaner Quantum Design PPMS9 magnetometer and its ACMS option.

Appendix A. Supplementary data

Additional magnetic data is electronically available. CCDC 2078711 and 2078827 contain the supplementary crystallographic data for (**1** and **1+2DMF**). These data may be obtained free of charge via http://www.ccdc.cam.ac.uk/conts/retrieving.html, or from the Cambridge Crystallographic Data Centre, 12 Union Road, Cambridge CB2 1EZ, UK; fax: +44 1223 336 033 or e-mail: deposit@ccdc.cam.ac.uk. Supplementary data to this article can be found online at https://doi.org/10.1016/j.poly.2021.115324.

References

[1] M. Shatruk, A. Dragulescu-Andrasi, K.E. Chambers, S.A. Stoian, E.L. Bominar, C. Achim, K.R. Dunbar, J. Am. Chem. Soc. 129 (2007) 6104.
[2] P.J. Ferko, S.M. Holmes, Curr. Inorg. Chem. 3 (2013) 172, and references cited therein.
[3] Y.-Z. Zhang, U.P. Malik, B. Quiggins, H. Nguyen, C.C. Beedle, A.E. Kovalev, R. Clérac, S. Hill, B.J. Bythell, S.M. Holmes, Eur. J. Inorg. Chem. 24 (2016) 2432, and references cited therein.
[4] S. Wang, X.H. Ding, J.-L. Zuo, X.-Z. You, W. Huang, Coord. Chem. Rev. 255 (2011) 1713, and references cited therein.
[5] R. Lescouëzec, J. Vaissermann, F. Lloret, F. Julve, M. Verdaguer, Inorg. Chem. 41 (2002) 5943.
[6] S. Wang, J.-L. Zuo, H.-C. Zhou, Y. Song, S. Gao, X.-Z. You, Eur. J. Inorg. Chem. (2004) 3681.
[7] Z.-H. Ni, H.-Z. Kou, L.-F. Zhang, W.-W. Ni, Y.-B. Jiang, A.-L. Cui, J. Ribas, O. Sato, Inorg. Chem. 44 (2005) 9631.
[8] S. Wang, J.-L. Zuo, H.-C. Zhou, Y. Song, X.-Z. You, Inorg. Chim. Acta 358 (2005) 2101.
[9] C.-F. Wang, Z.-G. Gu, X.-M. Lu, J.-L. Zuo, X.-Z. You, Inorg. Chem. 47 (2008) 7957.
[10] D.-F. Li, R. Clérac, S. Parkin, G.-B. Wang, G.T. Yee, S.M. Holmes, Inorg. Chem. 45 (2006) 5251.
[11] Y.-Z. Zhang, D.-F. Li, R. Clérac, S.M. Holmes, Polyhedron 60 (2013) 110.
[12] C.C. Beedle, Y.-Z. Zhang, S.M. Holmes, S. Hill, S. Polyhedron 59 (2013) 48.
[13] Y.-Z. Zhang, U.P. Mallik, N.P. Rath, R. Clérac, S.M. Holmes, Inorg. Chem. 50 (2011) 10537.
[14] Z.-H. Ni, L.-F. Zhang, C.-H. Ge, A.-L. Cui, H.-Z. Kou, J. Jiang, Inorg. Chem. Commun. 11 (2008) 94.
[15] D.F. Li, S. Parkin, G.B. Wang, G.T. Yee, A.V. Prosvirin, S.M. Holmes, Inorg. Chem. 44 (2005) 4903.
[16] D. Li, S. Parkin, G. Wang, G.T. Yee, S.M. Holmes, Inorg. Chem. 45 (2006) 1951.
[17] C.-F. Wang, W. Liu, Y. Song, X.-H. Zhou, J.-L. Zuo, X.-Z. You, Eur. J. Inorg. Chem. (2008) 717.
[18] Y.-Z. Zhang, U.P. Mallik, R. Clérac, N.P. Rath, S.M. Holmes, Polyhedron 52 (2013) 115.
[19] W. Liu, C.-F. Wang, Y.-Z. Li, J.-L. Zuo, X.-Z. You, Inorg. Chem. 45 (2006) 10058.
[20] L. Jiang, X.L. Feng, T.B. Lu, S. Gao, Inorg. Chem. 45 (2006) 5018.
[21] Z.-G. Gu, Q.-F. Yang, X.-H. Zhou, J.-L. Zuo, X.-Z. You, Inorg. Chem. 46 (2007) 3236.
[22] Y.-Z. Zhang, U.P. Mallik, R. Clérac, N.P. Rath, S.M. Holmes, Chem. Commun. 47 (2011) 7194.
[23] D. Li, S. Parkin, G. Wang, G.T. Yee, R. Clérac, W. Wernsdorfer, S.M. Holmes, J. Am. Chem. Soc. 128 (2006) 4214.
[24] Y.-Z. Zhang, U.P. Mallik, N.P. Rath, G.T. Yee, R. Clérac, S.M. Holmes, Chem. Commun. 46 (2010) 4953.
[25] D.-F. Li, S. Parkin, R. Clérac, S.M. Holmes, Inorg. Chem. 45 (2006) 7569.
[26] M. Nihei, M. Ui, N. Hoshino, H. Oshio, Inorg. Chem. 47 (2008) 6106.
[27] J.-R. Jiménez, J. Glatz, A. Benchohra, G. Gontard, L.-M. Chamoreau, J.-F. Meunier, A. Bousseksou, R. Lescouëzec, Angew. Chem. Int. Ed. 59 (2020) 8089.
[28] D.-F. Li, R. Clérac, O. Roubeau, E. Harté, C. Mathonière, R. Le Bris, S.M. Holmes, J. Am. Chem. Soc. 128 (2008) 252.
[29] D. Ganier, J.-R. Jiménez, Y. Li, J. von Bardeleben, Y. Journaux, T. Augenstein, E.M. B. Moos, M.T. Gamer, F. Breher, R. Lescouëzec, Chem. Sci. 7 (2016) 4825.
[30] Y.-Z. Zhang, P. Ferko, D. Siretanu, R. Ababei, N.P. Rath, M.J. Shaw, R. Clérac, C. Mathonière, S.M. Holmes, J. Am. Chem. Soc. 136 (2014) 16854.
[31] Y.-Z. Zhang, D.-F. Li, R. Clérac, M. Kalisz, C. Mathonière, S.M. Holmes, Angew. Chem., Int. Ed. 49 (2010) 3752.
[32] M. Nihei, Y. Sekine, N. Suganami, H. Oshio, Chem. Lett. 39 (2010) 978.
[33] R. Clérac, H. Miyasaka, M. Yamashita, C. Coulon, J. Am. Chem. Soc. 124 (2002) 12837.
[34] C.-F. Wang, D.-P. Li, X. Chen, X.-M. Li, Y.-Z. Li, J.-L. Zuo, X.-Z. You, Chem. Commun. 45 (2009) 6940.
[35] T. Liu, H. Zheng, S. Kang, Y. Shiota, S. Hayami, M. Mito, O. Sato, K. Yoshizawa, S. Kanegawa, D.A. Chunying, Nat. Comm. 4 (2013) 2826.
[36] T. Liu, Y.-J. Zhang, S. Kanegawa, O. Sato, J. Am. Chem. Soc. 132 (2010) 8250.
[37] Y.-J. Zhang, T. Liu, S. Kanegawa, O. Sato, J. Am. Chem. Soc. 132 (2010) 912.
[38] S. Trofimenko, Scorpionates. The Coordination Chemistry of Polypyrazolylborate Ligands, Imperial College Press, London, 1999 and references cited therein.
[39] D. Siretanu, D.-F. Li, L. Buisson, D.M. Bassani, S.M. Holmes, C. Mathonière, R. Clérac, Chem. Eur. J. 17 (2011) 11704.
[40] M. Nihei, Y. Sekine, N. Suganami, K. Nakazawa, A. Nakao, Y. Murakami, H. Oshio, J. Am. Chem. Soc. 113 (2011) 3592.
[41] A. Mondal, Y. Li, M. Seuleiman, M. Julve, L. Toupet, L.M. Buron-Le Cointe, R. Lescouëzec, J. Am. Chem. Soc. 135 (2013) 1653.
[42] Y. Sekine, M. Nihei, R. Kumai, H. Nakao, Y. Murakimi, H. Oshio, Chem. Commun. 50 (2014) 4050.
[43] Y. Sekine, M. Nihei, R. Kumai, H. Nakao, Y. Murakimi, H. Oshio, Inorg. Chem. Front. 1 (2014) 540.
[44] C. Zheng, J. Xu, Z. Yang, J. Tao, D. Li, Inorg. Chem. 54 (2015) 9687.
[45] K.E. Funck, M.G. Hilfiger, C.P. Berlinguette, M. Shatruk, W. Wernsdorfer, K. R. Dunbar, Inorg. Chem. 48 (2009) 3438, and references cited therein.
[46] M.A. Halcrow, K.R. Dunbar, C. Achim, M. Shatruk, Charge Transfer-Induced Spin-Transitions in Cyanometalate Materials, Wiley, New York, 2013 and references cited therein.
[47] C. Mathonière, Eur. J. Inorg. Chem. (2018) 248.
[48] K. Park, S.M. Holmes, Phys. Rev. B 74 (2006), 224440.
[49] S. De, A. Flambard, D. Garnier, P. Herson, F.H. Köhler, A. Mondal, K. Costuas, B. Gillon, R. Lescouëzec, B. Le Guennic, F. Gendron, Chem. Eur. J. 25 (2019) 12120.
[50] A.S. Felts, A. Slimani, J.M. Cain, M.J. Andrus, A.R. Ahir, K.A. Abboud, M. W. Meisel, K. Boukheddaden, D.R. Talham, J. Am. Chem. Soc. 140 (2018) 5814.
[51] Y. Moritomo, K. Kato, A. Kuriki, M. Takata, M. Sakata, H. Tokoro, S. Ohkoshi, K. Hashimoto, J. Phys. Soc. Jpn. 71 (2002) 2078.
[52] E.J.M. Vertelman, T.T.A. Lummen, A. Meetsma, M.W. Bouwkamp, G. Molnar, P.H. M. van Loosdrecht, P.J. van Konigsbruggen, Chem. Mater. 20 (2008) 1236.
[53] G. Molnár, S. Cobo, T. Mahfoud, E.J.M. Vertelman, P.J. van Konigsbruggen, P. Demont, A. Bousseksou, J. Chem. Phys. C 113 (2009) 2586.
[54] J.-H. Her, P.W. Stephens, C.M. Kareis, J.S. Moore, K.S. Min, J.-W. Park, G. Bali, B. S. Kennon, J.S. Miller, Inorg. Chem. 49 (2010) 1524.
[55] H. Tokoro, S.-I. Ohkoshi, Dalton Trans. 40 (2011) 6825, and references cited therein.
[56] S.-I. Ohkoshi, H. Tokoro, Acc. Chem. Res. 45 (2012) 1749.
[57] A. Bleuzen, V. Marvaud, C. Mathonière, B. Sieklucka, M. Verdaguer, Inorg. Chem. 48 (2009) 3453, and references cited therein.
[58] C. Tian, E. Kan, C. Lee, M.-H. Whangbo, Inorg. Chem. 49 (2010) 3086.
[59] Z.-H. Ni, H.-Z. Kou, Y.-H. Zhao, L. Zheng, R.-J. Wang, A.-L. Cui, O. Sato, Inorg. Chem. 44 (2005) 2050.
[60] A. Panja, P. Guionneau, I.-R. Jeon, S.M. Holmes, R. Clérac, C. Mathonière, Inorg. Chem. 51 (2013) 12350.
[61] D. Zhang, H. Wang, Y. Chen, Z.-H. Ni, L. Tian, J. Jiang, Inorg. Chem. 48 (2009) 5488.
[62] D. Dong, Y. Zhang, C. Jiao, L. Zhao, T. Liu, D. Liu, Z. Li, J. Liu, D. Liu, New J. Chem. 40 (2016) 8451.
[63] L.M. Toma, J. Pasán, C. Ruiz-Pérez, F. Lloret, M. Julve, Dalton Trans. 41 (2012) 13716.
[64] J. Kim, S. Han, I.-K. Cho, K.Y. Choi, K.Y.M. Heu, S. Yoon, B.J. Suh, Polyhedron 23 (2004) 1333.
[65] S.M. Holmes, Molecule-Based Magnets Constructed from Hexacyanometalates, Ph. D. Thesis, University of Illinois at Urbana-Champaign, Urbana, IL, 1999.
[66] E.A. Boudreaux, L.N. Mulay, Theory and Applications of Molecular Paramagnetism, 1976, pp. 491-496, Wiley, NY.
[67] G.M. Sheldrick, SHELX-97, Programs for Crystal Structure Solution and Refinement, University of Göttingen, Göttingen, Germany.
[68] G.M. Sheldrick, Acta Crystallogr. A 64 (2008) 112.
[69] G.M. Sheldrick, SADABS, An empirical absorption correction program, Bruker Analytical X-ray Systems, Madison, WI, 1996.
[70] International Tables for Crystallography, vol. C, Kluwer Academic Publishers, Dordrecht, Netherlands, 1992.
[71] K. Nakamoto, Infrared and Raman Spectra of Inorganic and Coordination Compounds, 5th ed.; Wiley: New York, 1997; Part B, pp 54–58 and 105–116.
[72] S.R. Choudhury, A. Dutta, S. Mukhopadhyay, L.P. Lu, M.L. Zhu, Acta Cryst. E62 (2006), m1489.
[73] S.A. Richert, P.K.S. Tsang, D.T. Sawyer, Inorg. Chem. 28 (1989) 2471.
[74] J.A. Smith, J.-R. Galán-Mascarós, R. Clérac, J.-S. Sun, X. Ouyang, K.R. Dunbar, Polyhedron 20 (2001) 1727.

[75] S.R. Holleman, O.J. Parker, G.L. Breneman, Acta Cryst. C50 (1994) 867.
[76] M. Wang, J. England, T. Weyermüeller, K. Weighardt, Inorg. Chem. 53 (2014) 2276.
[77] N.F. Chilton, R.P. Anderson, L.D. Turner, A. Soncini, K.S. Murray, J. Comput. Chem. 34 (2013) 1164.
[78] J. Goodenough, Magnetism and the Chemical Bond, Wiley, New York, 1963.
[79] R. Lescouëzec, F. Lloret, M. Julve, J. Vaissermann, M. Verdaguer, Inorg. Chem. 41 (2002) 818.
[80] S. Tanase, M. Andruh, N. Stanica, C. Mathonière, G. Rombaut, S. Golhen, L. Ouahab, Polyhedron 22 (2003) 1315.
[81] R. Sessoli, D. Gatteschi, Angew. Chem., Int. Ed. 42 (2003) 268.